As the aperture increases until 75-80%, a linear region is observed, due to an increasing excitation of the TE_0 mode. It can be observed, however, that at 50% aperture, normalized power is not at 0.5, but at an approximate value of 0.3. Since it could seem confusing that when waveguides are half covered normalized power is not 1/2, a second set of simulations were done. Showed in dashed points at fig. 4.34b, two waveguides without separation between them were considered and an extremely absorbent media was placed at a given distance z_0 partially covering the light path. Results show that when the waveguides do not have a gap between them, a significant broadening of the linear region is observed and that at 50% aperture, the expected 0.5 normalized power is obtained. Thence, it can be concluded that beam broadening in the free space is an important factor that should be taken into account on the design, since it modifies the span. In turn, it also means that diaphragm dimension in the z direction should be as small as possible, in order to reduce beam divergence. Thus, considering the silicon absorption coefficient, an agreement must be reached between the amount of light power that should be attenuated by the diaphragm and its dimensions in the z-axis. The working linear region and the diaphragm position that provides with 0.5 normalized power will depend on this agreement. This point is extremely important since if the initial aperture is chosen so as to provide ½ of normalized power, it will be then possible to distinguish between positive and negative acceleration with the same working range. For values above 75-80%, an expectable saturation regime is observed. It can be seen that power unity is never obtained. This is mainly due to the fact that although input and output waveguides have different widths, its core height is identical. Thus, again due to beam divergence, but this time in the *y*-axis, even if diaphragm is fully open, there always exists a fraction of the light that will not be coupled into the output waveguide.

Then, the linear working region for a 30μm width diaphragm between two waveguides distanced 50μm is located between 35% and 75% of diaphragm aperture, which means a movement range of 1.6μm (0.8μm in each direction). This working range is much larger operation range as compared to standard TIR optical accelerometers **[25]**. According to the slope of this working region, an optical sensitivity of 9dB/g should be obtained. Depending on the design of the beams and the

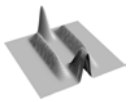

seismic mass, this large optical sensitivity would allow precise acceleration determination over a small acceleration range or, equivalently, ability to measure over a large range of accelerations. The requested specifications for this concrete accelerometer correspond to the second possibility, since it was expected to measure up to 50g in the linear range. It would also be of worth knowing the failure losses, that is, the amount of power lost when the accelerometer mass is broken for self-test purposes. Due to its working principle, having the diaphragm fully open or not having the diaphragm should bring the same results. Since waveguides are relatively closer, the failure losses are negligible in *x* direction and are 0.23dB in the *y*-axis.

Once the linear region and the expected maximum acceleration to be measured are known, mechanical parts of the device have to be accurately designed so as to match with the optical requirements. Concretely, the size of the mass, together with the geometry and position of the beams are the main factors that provides the accelerometer with the expected sensitivity. Mechanical optimization has been done using the commercially available finite-element method ANSYS v5.7 program, in its full version. From the analytical expressions and the simulations, it has been possible to analyze the beam mechanical stresses and the mass displacements for accelerations in the three axis. The structure vibrational modes and their frequencies have also been obtained. The main objective was the design of a micromechanical structure that had a span of 1μm in the z-axis when submitted to a given acceleration ρ in the same direction, that is, having a sensitivity of 1/ρ (μm/g). Although our linear region is larger than these requested specifications, limiting the range to 0.5μm around the stability point would assure to work in the linear region even if the seismic mass was slightly displaced without acceleration.

The diaphragm has been considered as fixed, that is, only the seismic mass has the possibility to be displaced. This simplification has been done due to the fact that the diaphragm has very small dimensions and a much higher natural frequency. Due to symmetry, the mass in a quad-bridge accelerometer configuration has a flat movement. This fact clearly simplifies the accelerometer design, since the total displacement will only depends on the geometry of the bridges. If the accelerometer had been based on cantilever structures, mass movement would not be flat and diaphragm final position

would be a function of the mass total size. Moreover, diaphragm would cover the waveguides with a tilt that would depend on the mass dimensions. Hence, quad-bridge configuration was chosen as optimum for optical accelerometer fabrication. According to the selected speed variation range, accelerometers were designed so as to have a vertical displacement of 0.5μm at 50 g. In fig 4.35a the mass displacement when the device is under an acceleration in the *y*-axis with a magnitude of 1g is presented. Fig. 4.35b and 4.35c shows the mass movement when the acceleration is produced in the other two axis (*z* and *x*-axes, respectively). In table 4.8 summarizes the mechanical results obtained. It can be seen that cross-accelerations values are significant and should be considered and controlled, since it could cause significant perturbations on the final accelerometer performances. Nevertheless, it can be observed that the center of the seismic mass in fig. 4.35c, that is, where the diaphragm is located, remains unperturbed when acceleration in *x*-axis is applied. Thence, cross acceleration in the *x*-axis can be neglected since it will cause no perturbation on the optical measurement.

Acceleration	Y_{max} (nm/g)	S_l (MPa)	S_t (MPa)
In y axis	10.2	20	2.3
In z axis	2.1		
In x axis	1.2*		

* For mass-centered diaphragm, there exists no movement.

Table 4.8: Maximum displacement in the *y*-axis (Y_{max}) for accelerations in the three directions and longitudinal and transversal mechanical stresses.

From the simulations, it can be seen that the parts that suffer from more bending during the acceleration measurement are the bridges. Then, it would be logical that they also had the highest mechanical stresses, caused by mass displacement. Generally, maximum mechanical stress that can be tolerated in silicon structures before breaking has been reported to be 6-9GPa **[26]**. Once it has been obtained the expected movement range for a given bridge, mechanical stresses at maximum deformation should be known in order to determine if the proposed bridge design would stand the mechanical stresses or, on the contrary, would broke for a given acceleration value.

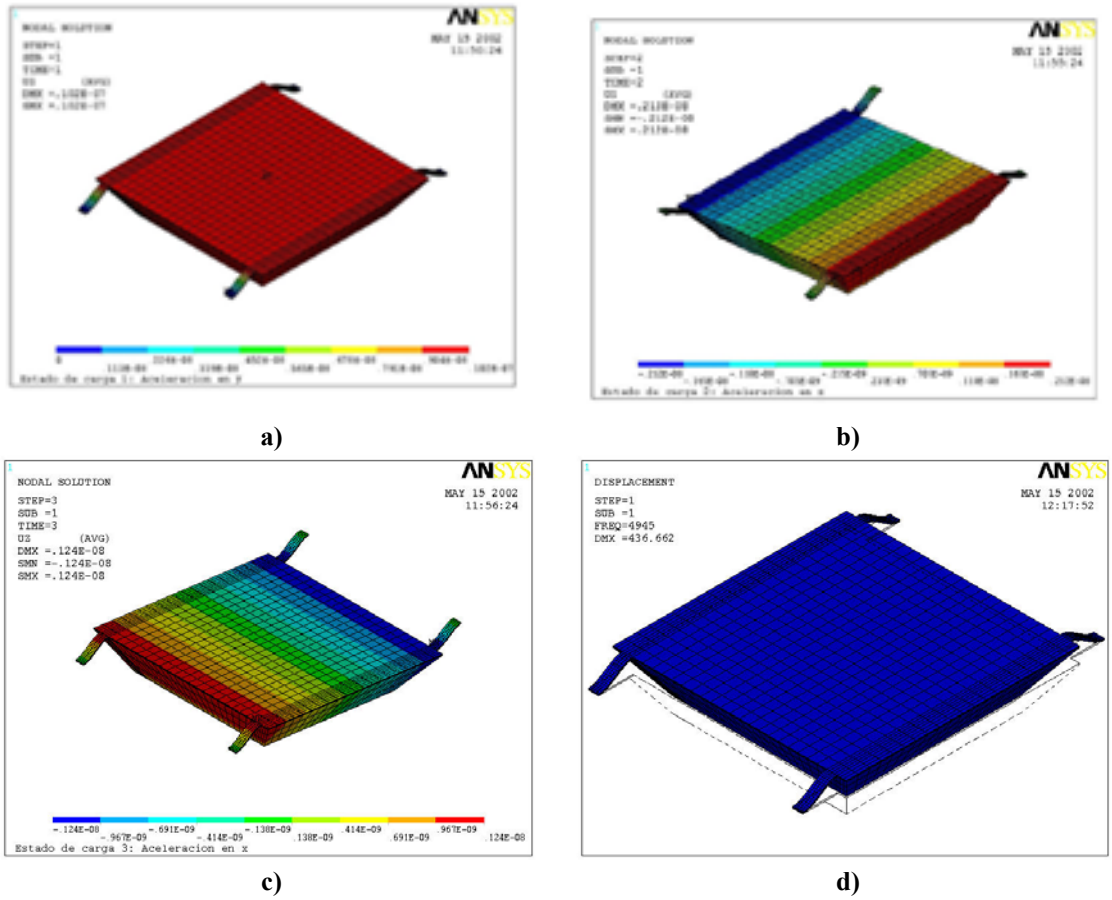

Fig 4.35. Displacement of the diaphragm accelerometer in the *y*-axis for an acceleration in the *y* axis a), in the *z* axis b) and in the *x* axis c). First vibrational mode is presented in d).

Simulations of the maximum mechanical stress longitudinal (S_l) and transversal (S_T) to the bridge are presented in fig. 4.36 (a and b, respectively), together with an averaged value considering a 3D motion. As can be observed, at 50g, the most important is the longitudinal stress, with a value of 20MPa. This result confirmed that the bridge was properly designed and that it would be able to measure the expected acceleration changes without reaching stress values close to the previously mentioned stress maximum value.

Finally, as it was highlighted in chapter 2, the resonant frequency is the limiting factor in the accelerometer application. Concretely, the lowest order mode, with a frequency of 4.945KHz, shown in fig 4.35d, determines the accelerometer working range.

Results from the previous optimization of the diaphragm accelerometer are summarized in table 4.9. Diaphragm optical accelerometer presents a large linear span,

which has been shortened so as to have an even more linear range and to assure working in the linear region even if a certain initial misalignment is produced. Failure losses are very low and matches with those corresponding to the fully open diaphragm. Thus, this latter value should be taken into account during the measurements, just in case that the seismic mass was broken and removed from the device. The high sensitivity that these accelerometers have in the linear region assures an optimum acceleration measurement. For that reason, they have been designed so as to measure up to 50g.

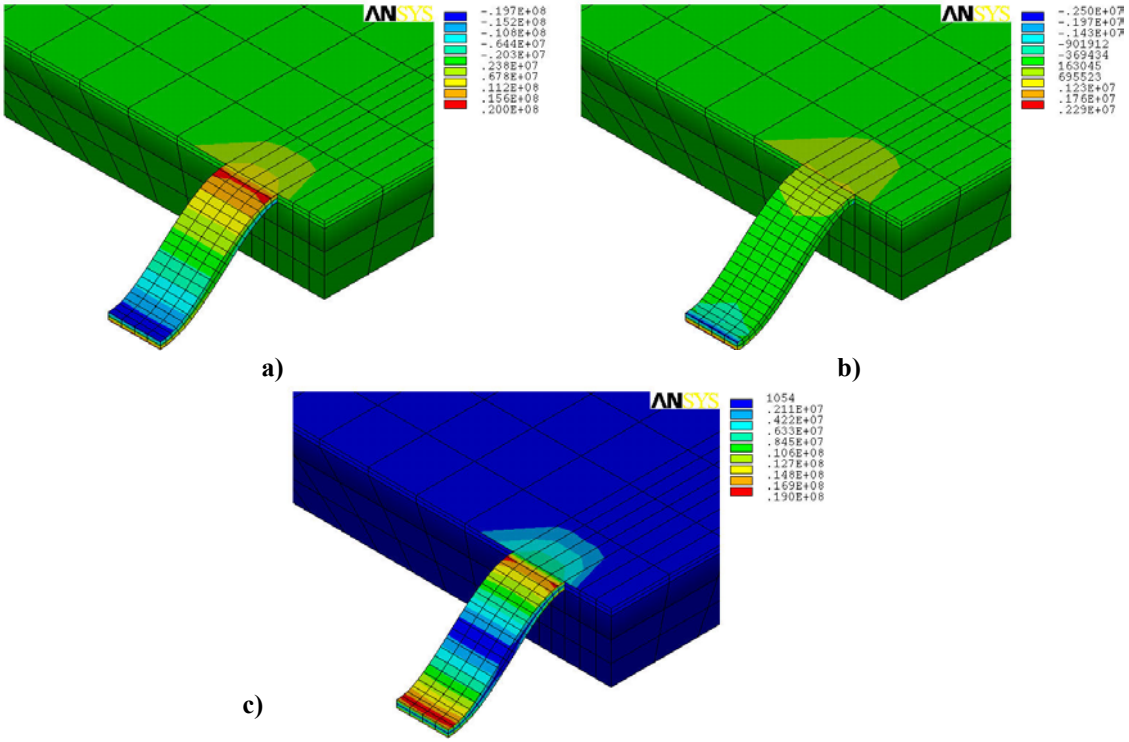

Fig 4.36. a) Lateral and b) transversal stress distribution on the bridges of the diaphragm accelerometer. c) Average stress value considering 3D movement.

As far as mechanical characterization is concerned, accelerometer geometry has been designed so as to fulfill the required diaphragm movement. It has to be noted that since the acceleration range is extremely large, the whole structure is extremely stiff. Accordingly, its natural frequency is also high. Crossed accelerations have been calculated and it has been noted that, due to the device design, only those in the *y*-axis should be considered during the measurement. Mechanical stresses are at utmost 0.3%

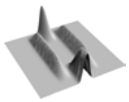

of the maximum stress permitted, confirming the correctness of the designed accelerometer.

Optical considerations

Waveguide width		Distance between waveguides (μm)	diaphragm width (μm)	Failure losses in z axis (dB)	Failure losses in x axis (dB)
Input (μm)	Output (μm)				
14	50	50	30	0.23	0

Mechanical considerations

Bridge Length (μm)	Top mass area (μm^2)	Sensitivity (dB/μm)	Frequency (KHz)	Span (μm)	Maximum displacement		
					x (nm/g)	z (nm/g)	y (nm/g)
365	2500x2500	9	4.945	1	0	2.1	10.2

Table 4.9. Basic specifications of the diaphragm-based optical accelerometer.

4.8 Misalignment Uniaxial Optical Accelerometer

As shown in fig. 4.37, the misalignment accelerometer basically consists on a three-fold segmented waveguide. The input and output waveguides are placed on the chip frame, while the sensing waveguide is located over the seismic mass. When a *y* acceleration is applied to the accelerometer, a double misalignment is produced, one at each cut. Distance between the seismic mass and frame has been reduced to 24μm, which is the minimum distance necessary to have a properly defined structure, according to technological parameters. From an optical point of view, this distance should be as short as possible in order to minimize light broadening. Nevertheless, maximum power transference between waveguides can be assured in the *x*-axis by ways of increasing its width at every step. Thus the first waveguide has a width of 14μm, the one in the middle has 30μm width and the output waveguide has 50μm.

Total losses as a function of the segmented waveguide misalignment caused by the seismic mass displacement were done identically as with the previous accelerometer, that is, by considering a cut in the y-z plane. Standard 4μm ARROW-A waveguides were also used. Fig 4.38a shows the propagating field across the

accelerometer when sensing waveguide is 50% misaligned as compared to input/output waveguides. Power at the waveguide output as a function of the seismic mass displacement (i.e. a double misalignment) without considering the insertion losses is presented in fig 4.38b: it is the highest when the three waveguides are aligned. If segments are progressively misaligned, either in +z or in –z direction, the power at the output progressively decreases. Thence, under this configuration it would not be possible to distinguish between positive and negative accelerations. However, a clear advantage as compared to the previously defined diaphragm accelerometer is observed: this configuration is self-aligned and has a very high failure losses in the *y* axis. Then, whether the seismic mass is broken, losses will be far out from the expected linear range, being easily detected at the device output.

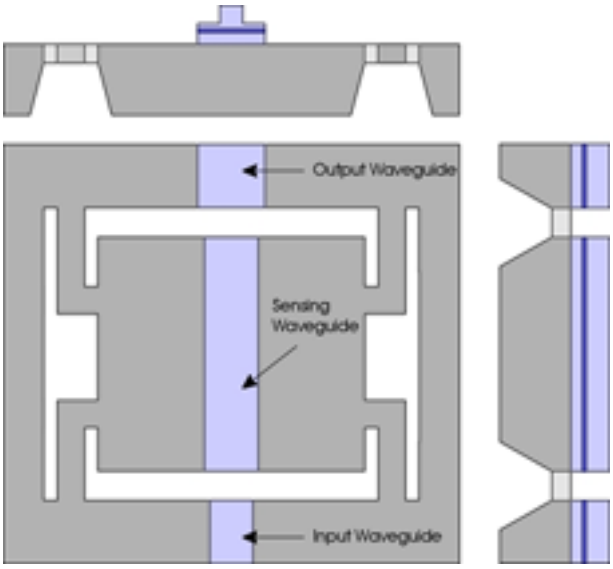

Fig 4.37. Scheme of the misalignment-based optical accelerometer.

Span was selected to be 2µm, with two linear zones located between [0.2, 1.0] µm and [-0.2,-1.0] µm (fig. 4.38b). Seismic mass were designed so as to reach maximum displacement in *y* axis at 1g. Thence, as opposite to the previous accelerometer, misalignment accelerometer has been designed so as to give an accurate acceleration value over a small acceleration range. As far as measurement is concerned, designing the device to work under 1g greatly simplifies its characterization, since by simply changing the device orientation in reference to the earth gravitational field the accelerometer response as a function of fractions of 1g will be achieved.